Experimental Research on Effects of Combustion Air Humidification on Energy and Environment Performance of a Gas Boiler

Experimental Research on Effects of Combustion Air Humidification on Energy and Environment Performance of a Gas Boiler

Qunli Zhang[1,2], Yanxin Li[1], Qiuyue Zhang[1], Qiu Shi[1], Xiaoshu Lü[3,4]

[1]Beijing Key Lab of Heating, Gas Supply, Ventilating and Air Conditioning Engineering, Beijing University of Civil Engineering and Architecture, Beijing 100044, China

[2]Collaborative lnnovation Center of Energy Conservation & Emission Reduction and Sustainable Urban-Rural Development in Beijing, Beijing 100044, China

[3]Department of Electrical Engineering and Energy Technology,
University of Vaasa, PO Box 700, Vaasa FIN-65101, Finland

[4]Department of Civil Engineering, Aalto University, PO Box 12100, Espoo FIN-02130, Finland

Abstract

To increase the waste heat recovery (WHR) efficiency of gas boiler and decrease NO_x emissions, a flue gas total heat recovery (FGTHR) system integrating direct contact heat exchanger (DCHE) and combustion air humidification (CAH) is put forward. The experimental bench and technical and economic analysis models are set up to simulate and evaluate the WHR performance and NO_x emissions in various operation situations. The results show that when the air humidity ratio elevates from 3 $g/kg_{dry\ air}$ to 60 $g/kg_{dry\ air}$, the dew point temperature increases by 7.9 °C. When the flue gas temperature approaches the dew point temperature, the rate of improvement of the FGTHR system's total heat efficiency notably rises. With spray water (SW) flowrate and temperature of 0.075 kg/s and 45 °C, the WHR efficiency relatively increases by up to 8.4%. The maximum sensible and latent heat can be recovered by 4468 w and 3774 w, respectively. The flue gas temperature can be reduced to 46.55 °C, and the average NO_x concentration is 39.6 mg/m^3. Compared with the non-humidified condition, the NO_x and CO_2 emissions relative reduction of the FGTHR system are 61.2% and 8.7%. The payback period of FGTHR system is 2 years. Through simulation, it can be concluded that the decrease in exhaust flue gas temperature and velocity, as well as the increase in exhaust flue gas humidity, has a negative impact on the diffusion of NO_x in the atmosphere.

Keywords:

air emissions from fossil fuel combustion, energy conversion/systems, energy systems analysis, fuel combustion, natural gas technology

1 Introduction

Due to global warming, climate issues are receiving increased attention from people [1]. More and more countries are announcing improvements in energy efficiency and reductions in greenhouse gas emissions to fulfill their obligations under the Paris Agreement [2]. However, increased CO_2 emissions from burning natural gas can lead to global warming [3]. In China, the demand for natural gas is expected to reach (5500–6500) × 10^8 m^3 around 2040,

an increase of 70% over 2020 [4,5]. The flue gas temperature without waste heat recovery (WHR) is about 150 °C [6], which consists of a sizable portion of water vapor with a significant quantity of latent heat [7,8]. Meanwhile, NO_x emissions in exhaust flue gas can cause negative environmental impacts such as acid rain, photochemical smog, and visual pollution [9,10].

Heat exchangers and heat pumps are utilized commonly in WHR systems [11,12]. Shang et al. [13] presented a non-direct contact heat exchange (non-DCHE) system whose energy conservation rate was 12.97% higher than an original boiler. Fluoroplastic non-direct heat exchange is used to overcome the corrosion problem, but it needs a bigger surface [14]. Conversely, the material consumption of DCHE is considerably less [15]. Due to the difficulty of cold sources at low temperatures faced by heat exchangers, the improvement of WHR efficiency is very limited [16]. Compared to the heat exchange technology, heat pumps utilize a low-grade heat source for recovering waste heat [17]. The lower the temperature of the cold source, the higher the WHR rate [18,19], which can rise to about 14% [20]. However, the coefficient of performance (COP) of absorption heat pumps decreases in cold regions due to the influence of evaporation temperature [21], and their initial investment is high [22].
At present, the methods for low-NO_x combustion technologies include premixed combustion [10], flue gas recirculation [23], staged combustion [24,25], and oxy-fuel combustion [26]. The inlet combustion air of the boiler is typically excessive to ensure adequate combustion. As a result, a significant amount of N_2 reacts with the remaining O_2 in the furnace to produce NO_x. By changing the state conditions of the gas inlet, such as premixed combustion, the problem of uneven furnace temperature caused by poor mixing can be effectively solved, and NO_x emissions can be reduced [27,28]. Injecting CO_2 [29], flue gas [30], H_2O [31], and other gases into the combustion chamber can inhibit the formation of NO_x. However, compared with water, the specific heat capacity of carbon dioxide and flue gas is large, and the thermal diffusivity is low. Excessive injection of CO_2 and flue gas can lead to combustion instability [32]. In contrast, water is a good choice, the increase in H_2O content effectively reduces the concentration of N_2 and O_2 in the air [33]. The endothermic process of H_2O in the furnace converts a large amount of combustion heat into latent heat for storage, reduces the combustion temperature in the furnace [34], and significantly inhibits the generation of NO_x.
In addition, although the NO_x pollutant concentration reaches the gas boiler emissions standard, terrible diffusion conditions can lead to NO_2 peak concentration exceeding air quality standards. The United States Environmental Protection Agency (EPA) used the 1-h standard indicator to protect public health by limiting people's exposure to short-term peak concentrations of NO_2. The EPA set a 1-h NO_2 standard of 100 parts per billion [35]. The Chinese ambient air quality standard (GB 3095-2012) allowed the maximum 1-h average value of NO_2 in residential ambient air functional area to be 250 $\mu g/m^3$ [36]. Compared to traditional boilers, changes in exhaust flue gas temperature, velocity, and humidity in the WHR system will affect the diffusion of pollutants.
In this paper, a collaborative flue gas total heat recovery (FGTHR) system was implemented to reduce NO_x emissions and improve WHR performance. The mathematical energy, environment, and economics models were established to compare different systems. The WHR efficiency and NO_x concentration effects under different air conditions were investigated by experimental setups. Quantitative comparative analysis was conducted on the DCHE system (single SW tower) and FGTHR system (double SW tower) to obtain suitable operating parameters for the SW tower. Subsequently, the effects of NO_x diffusion in the exhaust gas at the stack exit were studied at different temperatures, velocities, and humidity. For the DCHE system, the temperature difference between the SW (spray water) and the flue gas was large, resulting in a decrease in the grade of recovered heat. The FGTHR system

consisted of DCHE and combustion air humidification (CAH) units to reduce each section's heat transfer temperature difference and the reduced grade of recovered heat. On the one hand, the FGTHR system solved the problem of finding a continuous low-temperature cold source and provided stable and sufficient environmental conditions for air preheating and humidification. On the other hand, air humidification changed the combustion temperature field, thus controlling pollutants.

2 Experiment and Method

2.1 System Description.

Figures 1 and 2 show the experimental system, which is composed of a gas boiler, two water tanks, a DCHE unit, a water–water heat exchanger, a CAH unit, and a water pump. The operating mode of the system could be adjusted using valves. The experimental system consists of four parts: the combustion air, the flue gas, the SW, and the heating water.

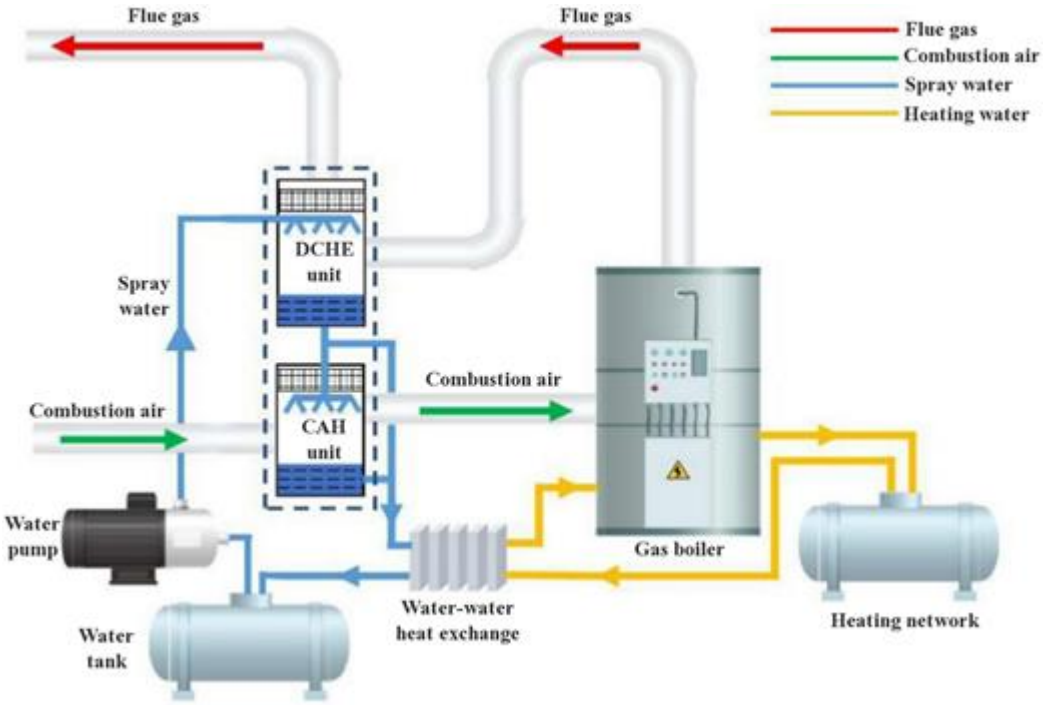

Fig. 1. Flow diagram of system

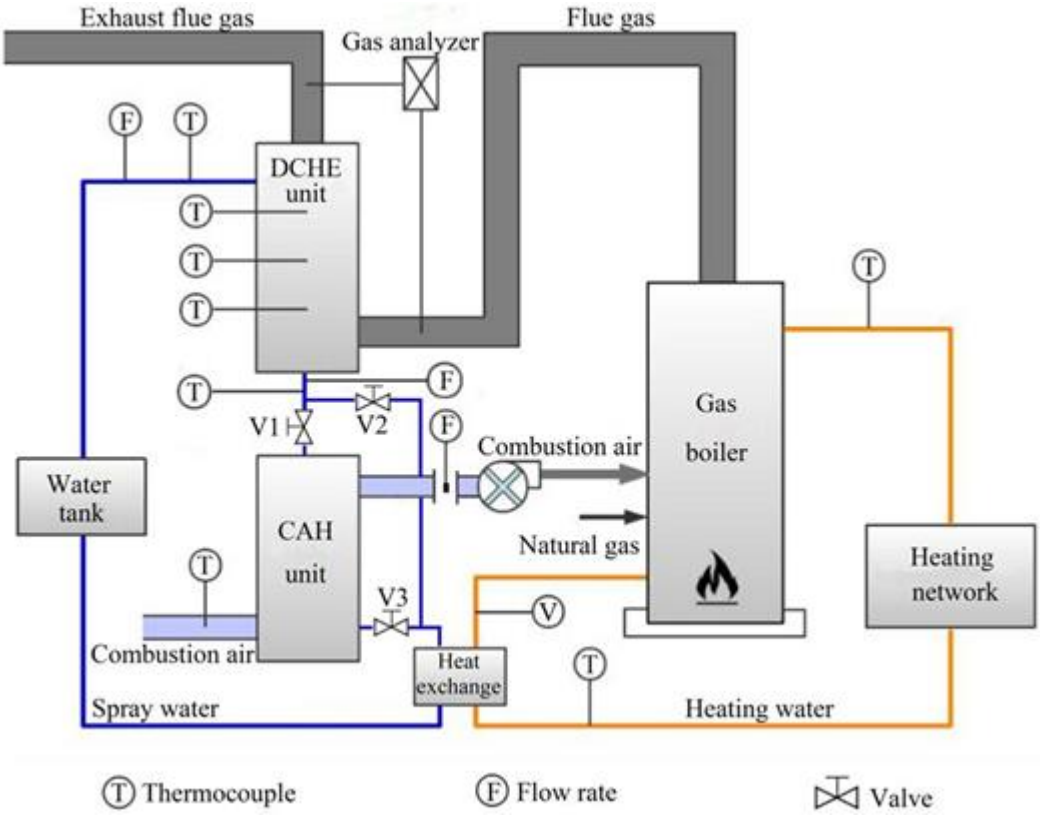

Fig. 2. Schematic chart of system and test point layout

FGTHR system mode: Valve 2 is closed, and valves 1 and 3 are opened.

1. Combustion air part: The air first enters the CAH unit, where it is converted to raise temperature and humidity before entering the gas boiler for natural gas combustion.
2. Flue gas part: Natural gas and air burn to form flue gas, which is entered into the DCHE unit to transfer heat. Then, the flue gas is discharged through the demist net.
3. SW cycle: As the SW reaches the DCHE unit, it is heated by the flue gas. Then, it enters the CAH unit to humidify the combustion air, and finally gain heat to the heat network's backwater via the heat exchanger.
4. Heating water part: The heat network is represented by a thermostatic water tank. The heat network's supply water recovers the heat of the SW via a heat exchanger, before being heated by the boiler and returned to the heating network to transfer heat to the consumer.

DCHE system mode: Valves 1 and 3 are closed, and valve 2 is opened. The flow of the flue gas, heating water, and combustion air parts is the same as in the FGTHR system mode.

1. SW cycle: As the SW reaches the DCHE unit, it is heated by the flue gas. Then, it gains heat to the heat network's backwater via the heat exchanger.

2.2 Test Methods and Instruments

2.2.1 Test Methods.

The arrangement of experimental instruments and test points are shown in Fig. 2. This experiment adopts the variable control method to explore the influence on the WHR quantity and NO_x emissions of the FGTHR system and DCHE system under different combustion air conditions, and water tank and water pump to control the DCHE unit SW temperature and flowrate. The SW flowrate of the DCHE and CAH units is the same. The experimental operating parameters are presented in Fig. 3.

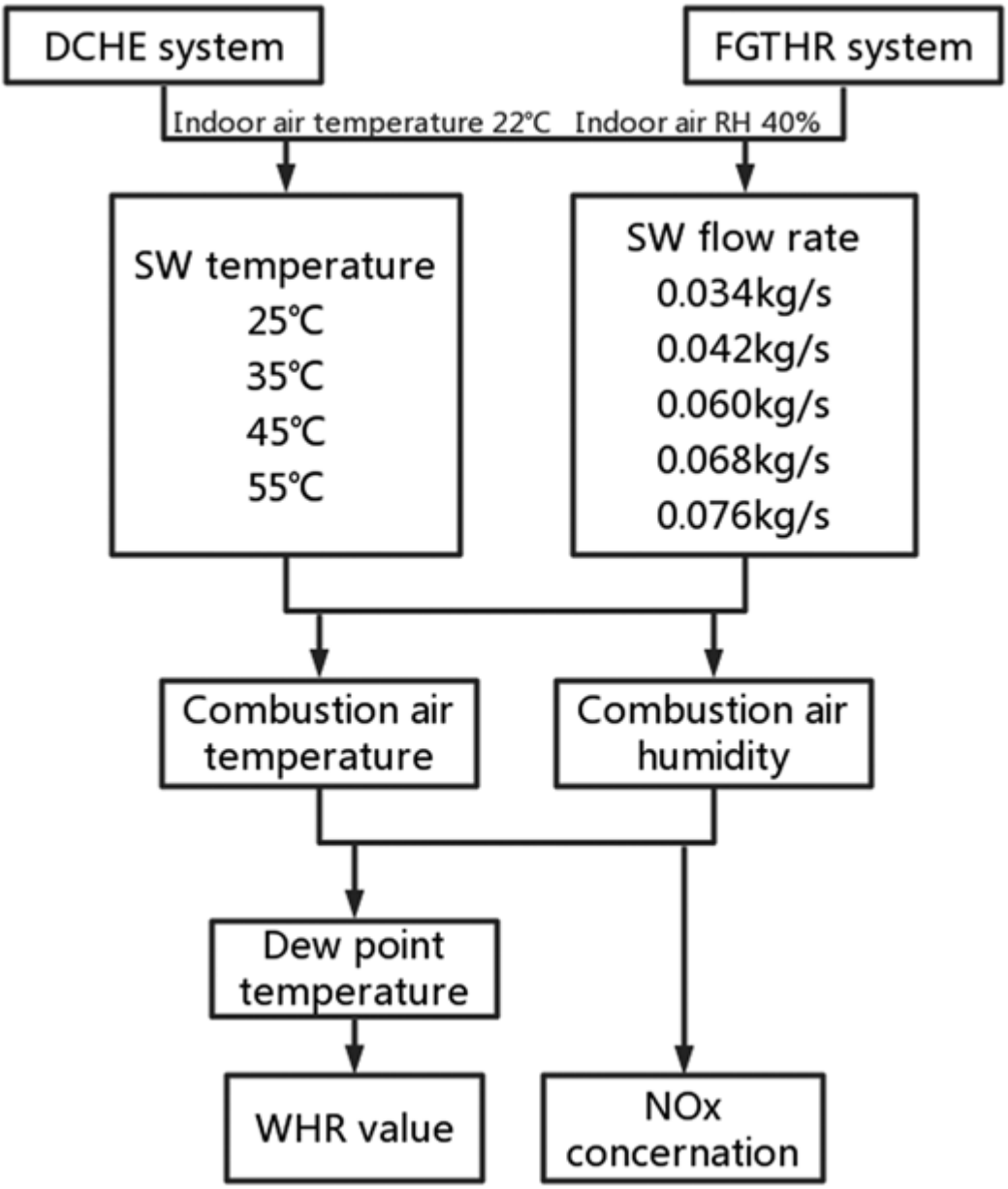

Fig. 3. Experimental conditions of system

2.2.2 Test Instruments.

This experiment was conducted in Beijing with an atmospheric pressure of 101.325 kPa. Instead of a gas boiler, this experiment used a Yingxue brand gas water heater (JSQ20). Table 1 lists the experimental gas boiler's basic parameters. This experiment used natural gas from Beijing city pipelines, where the low calorific value ranged at 35.34 MJ/Nm^3. The parameters of test apparatuses are listed in Table 2.

Table 1 Basic parameters of gas boiler

Equipment parameters	**Value**
The rated heat load	58 kW
Natural gas consumption	5.2 Nm^3/h
Flue gas temperature	180 °C
Rated inlet/outlet water temperature	85 °C/65 °C
Feedwater temperature	18 °C
Boiler load	90%
Heat transfer area	2.1 m^2
Excess air ratio	1.4

Table 2 Test bench major apparatuses and precision

Table 2 Test bench major apparatuses and precision

Measure parameters	Apparatuses	Type	Manufacturer	Precision
Flue gas temperature	Gas analyzing device	Testo 340	Testo, Germany	±0.5%
SW Temperature	Thermocouple	Omega K	OMEGA Engineering Inc., America	±0.75%
Air temperature	Thermocouplè	Omega K	OMEGA Engineering Inc., America	±0.75%
NO Concentration	Gas analyzing device	Testo 340	Testo, Germany	±5 ppm
NO_2 Concentration	Gas analyzing device	Testo 340	Testo, Germany	±10 ppm
O_2 Concentration	Gas analyzing device	Testo 340	Testo, Germany	±0.2%
SW Flowrate	Rotameter	SKLZBY-15MT	Jiangsu Suke Instrument Inc., China	±4%
Air flowrate	Orifice flowmeter	IRIS 100	Emile Egger, Switzerland	±1.5%
Air humidity ratio	Humidity self-recording instrument	WWSZY-1	Beijing Hongou Chengyun Instrument Inc., China	±2%
Data collection	Data receiver	Agilent 34970A	Agilent Technologies Inc., America	±0.004%

2.3 Technical and Economic Analysis

2.3.1 Energy Models

(1) Gas composition models

To clarify the use of moist air in boilers, main gas composition equations are used to calculate:

$$V_{fg} = V_{N2} + V_{wp}^{o} + V_{RO_2}^{o} + V_{O_2} \quad (1)$$

$$V_{N2}^{o} = 0.01N_2 + 0.79\alpha V_{ng}^{o} \quad (2)$$

$$V_{wp}^{o} = 0.01(2CH_4 + 4C_3H_8 + 0.12d_a) + 0.0016d_{ng}V_{ng}^{0} \quad (3)$$

$$V_{RO_2}^{o} = 0.01(CO_2 + CH_4 + 3C_3H_8) \quad (4)$$

$$V_{O2} = (\alpha - 1)V_{ng}^{o} \quad (5)$$

where V_{fg}, $V_{RO2}{}^{O}$, and V_{O2} are the volume of flue gas, triatomic gas, and oxygen gas, m^3/m^3; V_{wp} and $V_{wp}{}^{O}$ are the water vapor volume at the inlet and outlet of the flue gas, m^3/Nm^3; α is the excess air ratio; d_{ng} and d_a are the natural gas and combustion air humidity ratios, $g/kg_{dry\ air}$.

(2) Thermal efficiency models

To better measure the heat and mass exchange of the system, the thermal efficiency equations have been established as follows:

$$Q_{in} = Q_{hw} + Q_{fg-sw} + Q_{fg} + Q_{loss} \quad (6)$$

$$Q_{in} = \frac{B \cdot Q_{net,ar}}{3600} \quad (7)$$

$$Q_{hw} = \eta_b \cdot Q_{ng} \quad (8)$$

$$Q_{fg-sw} = c_w m_w (t_2 - t_1) \quad (9)$$

$$Q_{SW-CA} = c_w m_w (t_3 - t_2) \quad (10)$$

$$\eta_b = \frac{Q_{hw}}{Q_{in}} \quad (11)$$

$$\eta_t = \frac{Q_{hw} + Q_{fg-sw}}{Q_{in}} \quad (12)$$

where Q_{in} is the heating power, kW; Q_{hw} is the heat intake by the heating network, kW; $Q_{fg\text{-}sw}$ is the heat gain from SW from the flue gas, kW; Q_{fg} is the heat emitted from exhaust flue gas, kW; Q_{loss} is the system's heat loss, kW; B is the natural gas consumption, Nm^3/h; $Qnet,ar$ is the low calorific value of natural gas, kJ/Nm^3; ηb is the boiler efficiency; ηt is the total heat efficiency of the gas boiler system; cw is the specific heat capacity, kJ/(kg · °C); mw is the mass flowrate of SW, kg/s; t_1 and t_2 are the inlet and outlet SW temperatures of the DCHE unit, °C; t_3 is the outlet SW temperature of CAH unit, °C.

2.3.2 Environmental Emissions Models.

Because natural gas for experiments does not contain sulfur, the environmental emissions of the system mainly include NO_x and CO_2. The calculation equations are as follows:

$$m_i = V_{fg} \cdot C_i \tag{13}$$

$$C_i = \frac{M_i \cdot C_{ppm,i}}{V_i} \tag{14}$$

where mi is the total emissions of i, mg/m^3; Ci is the mass concentration of i, mg/m^3; Mi is the relative molecular mass of i; $C_{ppm,i}$ is the parts per million (PPM) concentration of i, mg/m^3.

2.3.3 Economic Model.

The calculation equation for the payback period is as follows:

$$P_t = \frac{I_t}{S_t - E_t} \tag{15}$$

where Pt is the payback period, a; Et is the cost of electricity, CNY; St is the cost-savings of natural gas, CNY; It is the initial investment of system, CNY.

2.4 Uncertainty Analysis.

The main uncertainty calculation formulas are shown in Table 3. According to the theory of error and data processing [37], the principal sources are the WHR quantity and NO_x concentration. The precision of test apparatuses is listed in Table 2. The following uncertainty is calculated based on the experimental condition of combustion air moisture content of 60 $g/kg_{dry\ air}$:

Table 3 Uncertainty calculation formulas

Uncertainty formula
$y=f(x_1, x_2, x_3, \cdots, x_n)$
$x_1=\bar{x}_1 \pm \Delta x_1, x_2=\bar{x}_2 \pm \Delta x_2, \cdots, x_n=\bar{x}_n \pm \Delta x_n$
$\Delta y=\sqrt{\left(\frac{\partial y}{\partial x_1}\Delta x_1\right)^2+\left(\frac{\partial y}{\partial x_2}\Delta x_2\right)^2+\left(\frac{\partial y}{\partial x_3}\Delta x_3\right)^2+\cdots+\left(\frac{\partial y}{\partial x_n}\Delta x_n\right)^2}$
$e=\frac{\Delta y}{y}\times 100\%$

The measurement uncertainty of inlet and outlet SW temperature are 0.3 °C and 0.4 °C. The relative uncertainty is 3.7%. Based on the measurement uncertainty of the mass flowrate of 4.0%, the related uncertainty of WHR is 5.6%. When the system was running steadily, the concentration NO_x was tested every 5 s. The measurement uncertainty of NO and NO_2 ppm concentration are 1.4 ppm and 1.6 ppm. The uncertainty of the NO_x concentration is 2.1 mg/m^3. The minimum and maximum NO_x concentrations are 38.3 mg/m^3 and 44.98 mg/m^3, respectively, with a relative uncertainty of 5.5%. Considering instruments and measurement errors, the mathematical models established in this study were dependable.

3 Results and Discussions

3.1 Energy Analysis

3.1.1 Dew Point Temperature Analysis.

The water dew point temperature in flue gas is mainly determined by the partial pressure of water vapor in the flue gas. The proportion of water vapor in the flue gas determines the partial pressure of water vapor. This section will mainly discuss the impact of air temperature and relative humidity on the water dew point of flue gas. The dew point temperature of flue gas under different combustion air conditions is shown in Fig. 4.

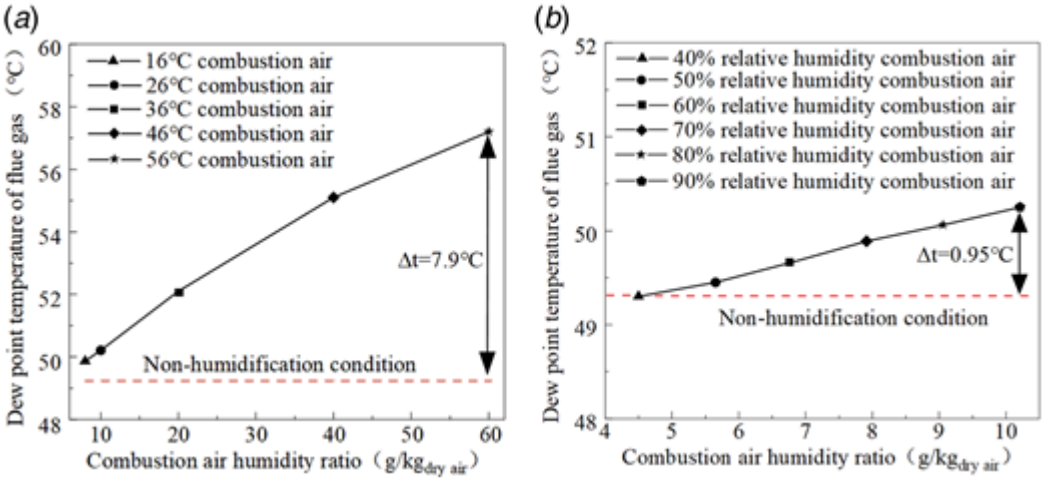

Fig. 4. Effect of air humidification on dew point temperature

Water produced during combustion makes up a portion of the water vapor, which also includes water from the air and natural gas. With the air humidity ratio increase, the water vapor volume, the corresponding pressure of water vapor, and the dew point temperature also

increase progressively. The dew point temperature was 49.3 °C under non-humidification conditions. The air humidity ratio varied greatly with the increase in air temperature. The dew point temperature goes up by 7.9 °C as the air humidity ratio reaches 60 $g/kg_{dry\ air}$.
The change in dew point temperature is only somewhat affected by the rise in air relative humidity. The change in dew point temperature is less affected by the air's relative humidity. The dew point temperature barely rises by 1 °C when the air's relative humidity is increased to 90%. Therefore, to increase the dew point of flue gas water, it is necessary to use a higher temperature water to humidify the combustion air.

3.1.2 Flue Gas Temperature Analysis.

In order to calculate the potential for WHR from boiler flue gas, the experimental boiler was used as an example to calculate the system heat efficiency of flue gas reduction to different temperatures after passing through a DCHE. Figure 5 depicts the outcomes of the calculations.

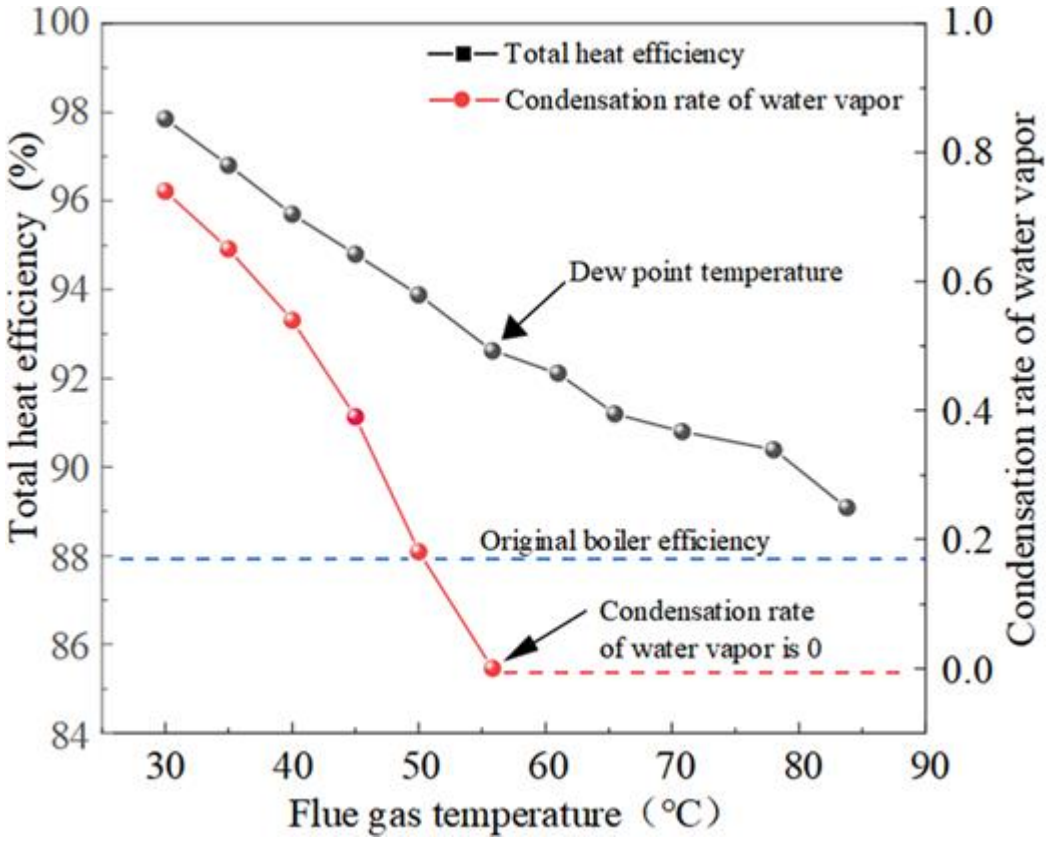

Fig. 5. Impact of flue gas temperature on total heat efficiency

Using the water vapor condensation rate (β) can also explain this phenomenon:

$$\beta = \frac{V_{wp} - V_{wp}^{o}}{V_{wp}} \qquad (16)$$

The β is zero at its dew point temperature (55 °C), and it remains constant as the flue gas temperature increases, both of which are zero. The total heat efficiency rises slowly at first (85–55 °C) and then quickly (55–30 °C). The turning point temperature is approximately 55 °C. The flue gas cooling process only releases its sensible heat above the dew point

temperature, and the quantity is lower. In contrast, the process releases a sizable amount of latent heat for temperatures below the dew point temperature. Therefore, raising the dew point temperature of flue gas by increasing the temperature and humidity of the air is a cost-effective method to achieve condensation of water vapor at higher temperatures, release a large amount of latent heat of vaporization, and then deeply recover the WHR of flue gas.

3.1.3 Waste Heat Recovery Performance Analysis

(1). WHR quantity of the DCHE system

First, research is conducted on the DCHE system under non-CAH conditions.

Figure 6 describes the relation between WHR quantity changes under different SW temperatures and SW flowrates. The WHR quantity gradually increases with the increase of SW flowrate.

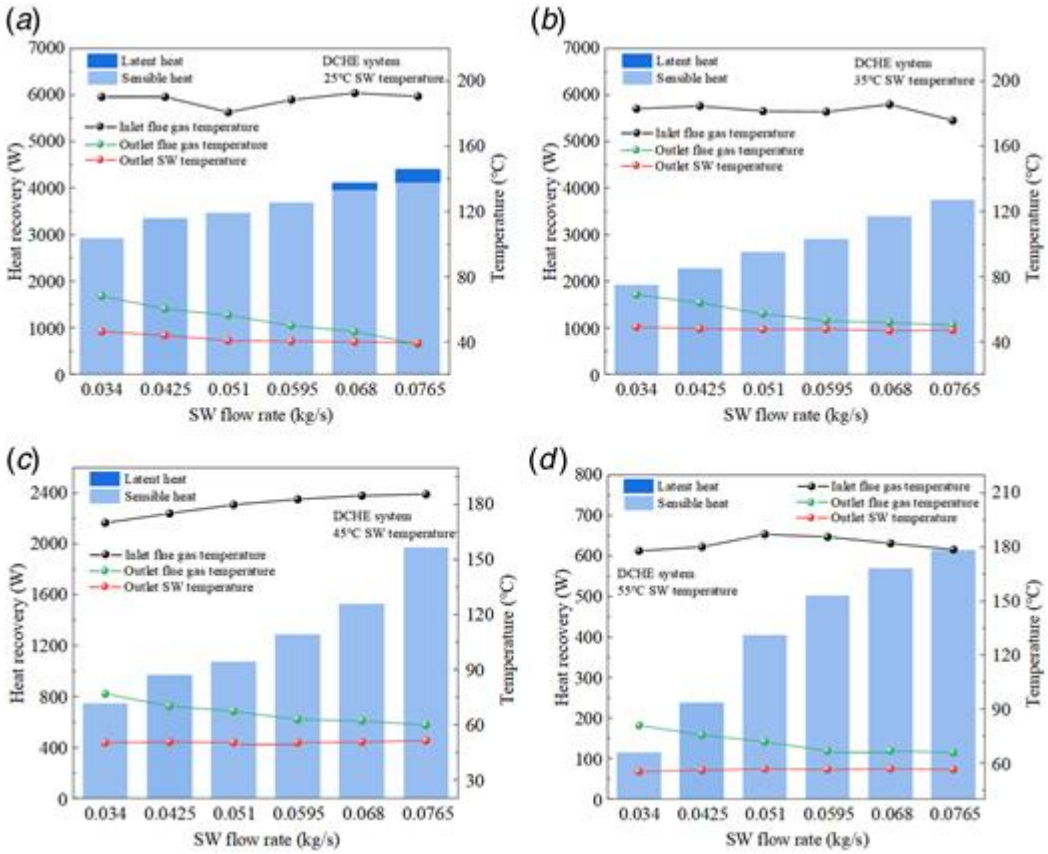

Fig. 6. Influence of WHR under different spary water temperatures and flowrates of DCHE system

When the SW flowrate is low, only a small portion of the sensible heat in the flue gas can be recovered. Increasing the SW flowrate can recover more heat from the flue gas, including latent heat in the flue gas. As the SW temperature increases, the WHR quantity gradually decreases, decreasing the latent heat recovery to zero. When the combustion air is not humidified, the WHR mainly recovers the sensible heat in the DCHE system. Considering the need for deep WHR, the FGTHR system is studied in the WHR quantity in the following section.

(2) WHR quantity of the FGTHR system

The relation between WHR quantity changes under different SW temperatures and SW flowrates of the FGTHR system was studied, as shown in Fig. 7. The overall trend of WHR quantity change is the same as that of the DCHE system. In contrast, the WHR rate of the FGTHR system is increased compared with the DCHE system. For example, at an SW temperature of 45 °C, the WHR rate of the FGTHR system has increased by 30%. Under the same SW rate, the FGTHR system can achieve the WHR that the DCHE system can recover at higher SW temperatures when the SW temperature is lower. As the SW temperature increases, latent heat reduces, indicating that a lower SW temperature can have a better WHR effect. When the SW temperature is the same, the rate of increase in latent heat becomes faster as the SW flowrate increases. But as the SW flowrate increases too much, the growth rate of WHR gradually slows down, and the effect on improving the WHR is limited.

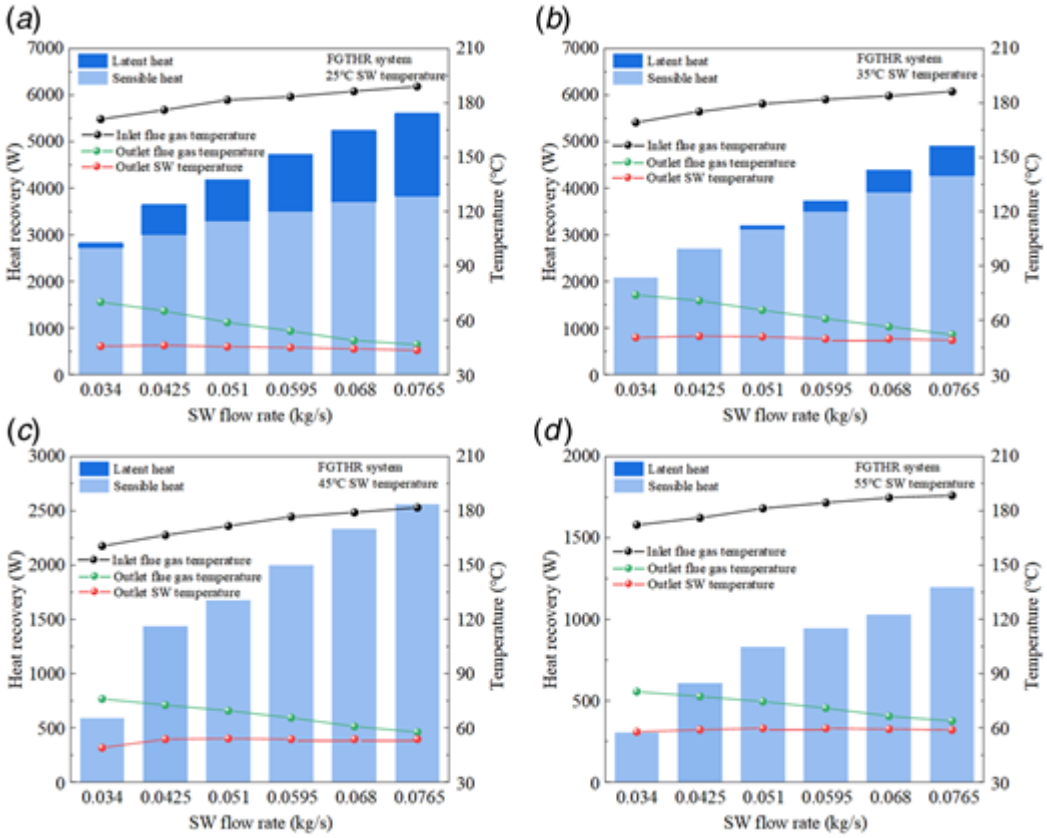

Fig. 7. Influence of WHR under different spray water temperatures and flowrates of FGTHR system

To better quantify the WHR quantity of the FGTHR system, we proposed using the moisture content of combustion air for analysis. Figure 8 shows the relationship between combustion air conditions under different SW flowrates and temperatures. As the SW flowrate and SW temperature increase, the temperature and humidity of the combustion air also increase. The maximum temperature of the combustion air can be increased to 47 °C, with a moisture content of 73 g/kg$_{\text{dry air}}$, notably increasing compared to the original indoor air.

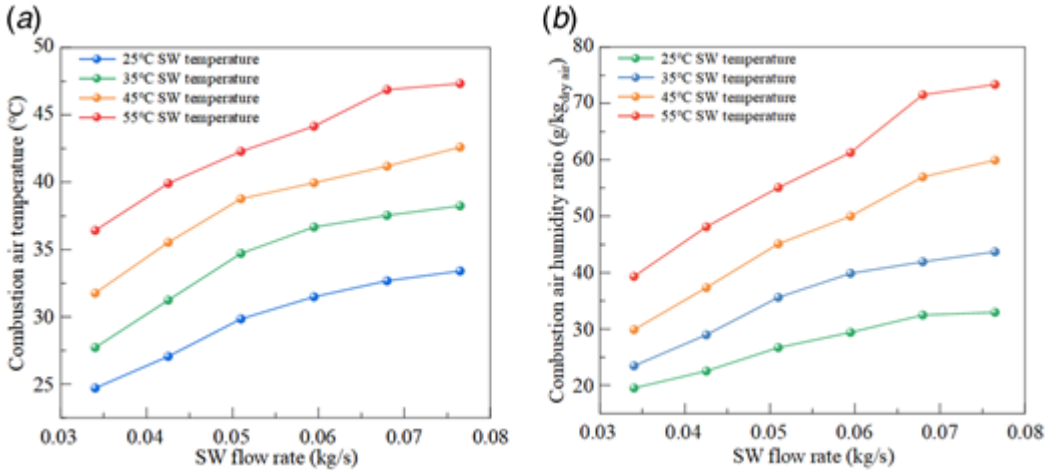

Fig. 8. The relationship between combustion air conditions under different spray water flowrates and temperatures

Figure 9 shows the influence of the combustion air humidity on WHR quantity. The latent heat recovery and flue gas dew point temperatures gradually rise as the combustion air's moisture content rises. Compared to the non-CAH condition (3 g/kg$_{dry\ air}$), the latent heat recovery and total WHR increased by 15% and 26%, respectively, at 60 g/kg$_{dry\ air}$ humidity.

(3) System heat efficiency analysis

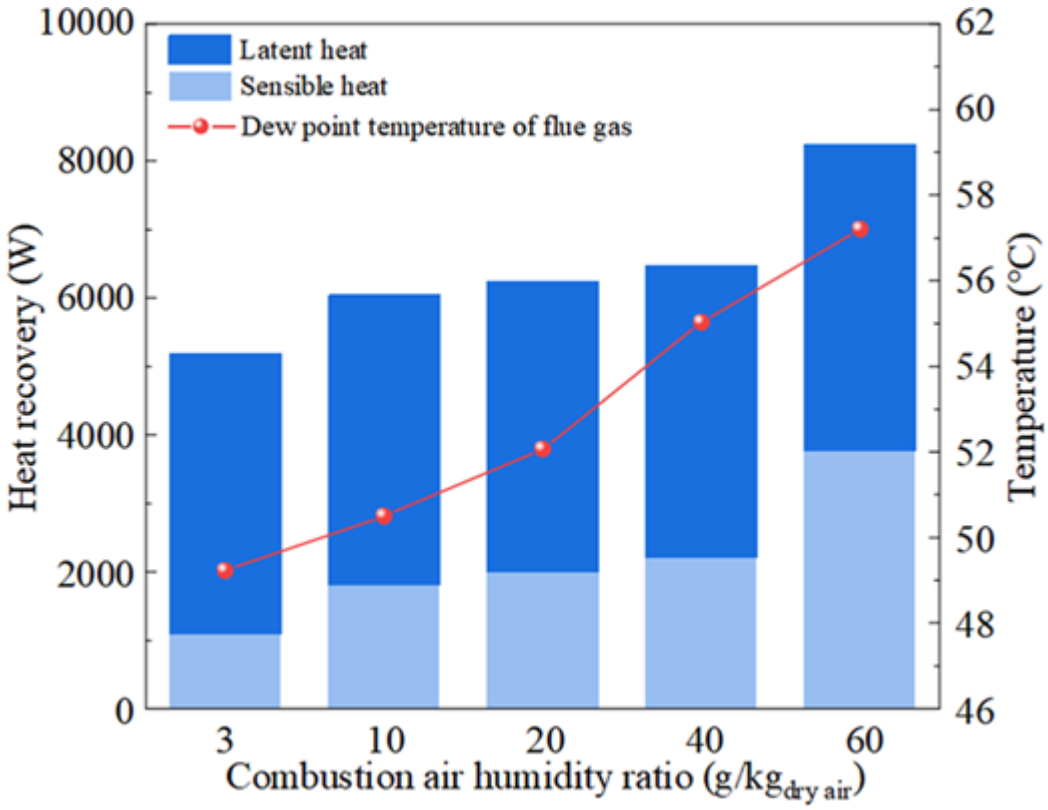

Fig. 9. The relationship between the waste heat recovery and the humidity of the combustion air

System heat efficiency is an essential assessment index. The heat efficiency of the different systems when generating 1 GJ of heat is listed in Table 4. Compared with the original system,

the FGTHR system saves 2.8 Nm^3 of natural gas, and the total heat efficiency relatively increased by 8.4%. The FGTHR system used 1.4 Nm^3 less natural gas than the DCHE system while increasing the heat efficiency by 3.9%. The experimental results show that air humidification can raise the WHR efficiency, and the FGTHR system has better energy efficiency.

Table 4. Comparison of three systems when generating 1 GJ of heat

Component	Original system	DCHE System	FGTHR System
Air humidity ratio ($g/kg_{dry\ air}$)	3	3	60
WHR efficiency (%)	0.0	3.9	8.4
System total heat efficiency (%)	88.0	91.9	96.4
Natural gas consumption (Nm^3)	32.2	30.8	29.4
Operating cost (CNY)	80.5	77.3	73.6

3.2 Economic Analysis.

The economic analysis compared operating costs when the different systems generated 1 GJ of heat. The electricity consumption of water pumps and fans and natural gas combustion account for the majority of the operating costs. Currently, the natural gas price in Beijing is 2.50 CNY/m^3 [38]. The economic comparison of the three systems is listed in Table 4. The operating expense of the FGTHR system is 6.9 CNY lower than that of the original system, which is a relative reduction of 8.6%. The operating cost of the FGTHR system is 3.7 CNY lower than that of the DCHE system, a relative reduction of 4.8%.

Compared to conventional boilers, FGTHR has additional WHR equipment. The costs of initial investment are shown in Table 5. According to Beijing's 120-day heating season, the natural gas savings and electricity cost for the entire heating season can be calculated, and the above two, along with the initial investment in the system, can be combined to obtain the payback period under the current operating condition. Figure 10 describes the economic analysis of different systems. The FGTHR system has twice the fuel savings and the same power consumption as the DCHE system. The FGTHR system's economic advantages will be greater if financial subsidies for clean combustion are taken into account.

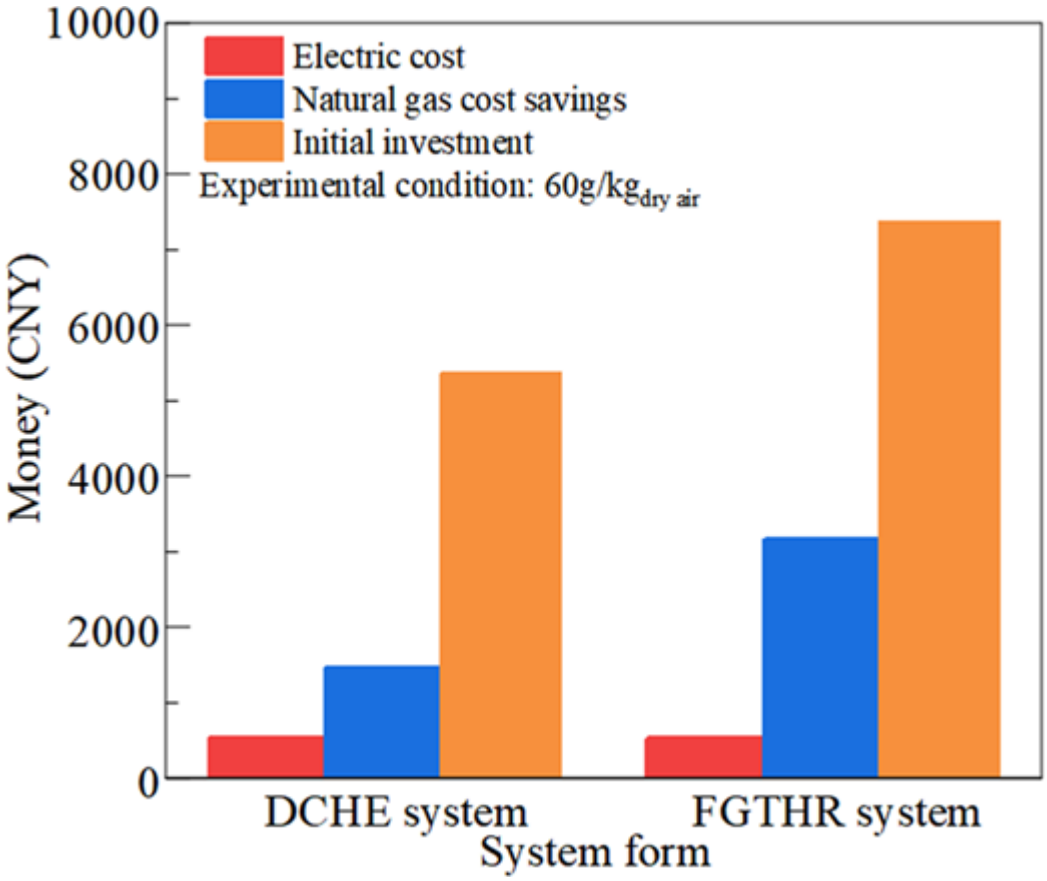

Fig. 10. System economic analysis

Table 5. Initial investment in equipment

Equipment	Quantity	Total price (CNY)
SW Tower	2	4000
Water–water heat exchange	1	500
Water pipes and fittings	Several	500
Water pump	1	750
Control system	1	850
Other	–	500
Total	–	7100

3.2 Environmental Emissions Analysis

(1) NO_x emissions

According to the different mechanisms, NO_x generated during combustion can be divided into fuel type, thermal type, and prompt type. The generation of fuel type NO_x is directly related to the N content in the fuel. The experimental natural gas with a 0.52% nitrogen

content can be ignored [39]. Temperature plays a decisive role in the production of thermal NO_x [40]. The thermal NO_x accounts for more than 90% of the total NO_x emissions [41]. Figure 11 shows the results, which reflect the trend of NO_x content in flue gas with time under different air humidity ratios. The NO_x emissions is 101.6 mg/m^3 under non-humidified condition. The NO_x emissions of the FGTHR system under the four air moisture levels are less than the emission standards. The NO_x concentration gradually decreases as the air humidity ratio rises. As the air humidity ratio is 60 g/kg$_{dry\ air}$, the NO_x emissions range from 38.3 mg/m^3 to 45.2 mg/m^3. The NO_x emissions average 39.6 mg/m^3, which is relatively reduced by 61.2%. The standard deviation of NO_x emissions is 1.3, indicating that the NO_x emissions are relatively stable.

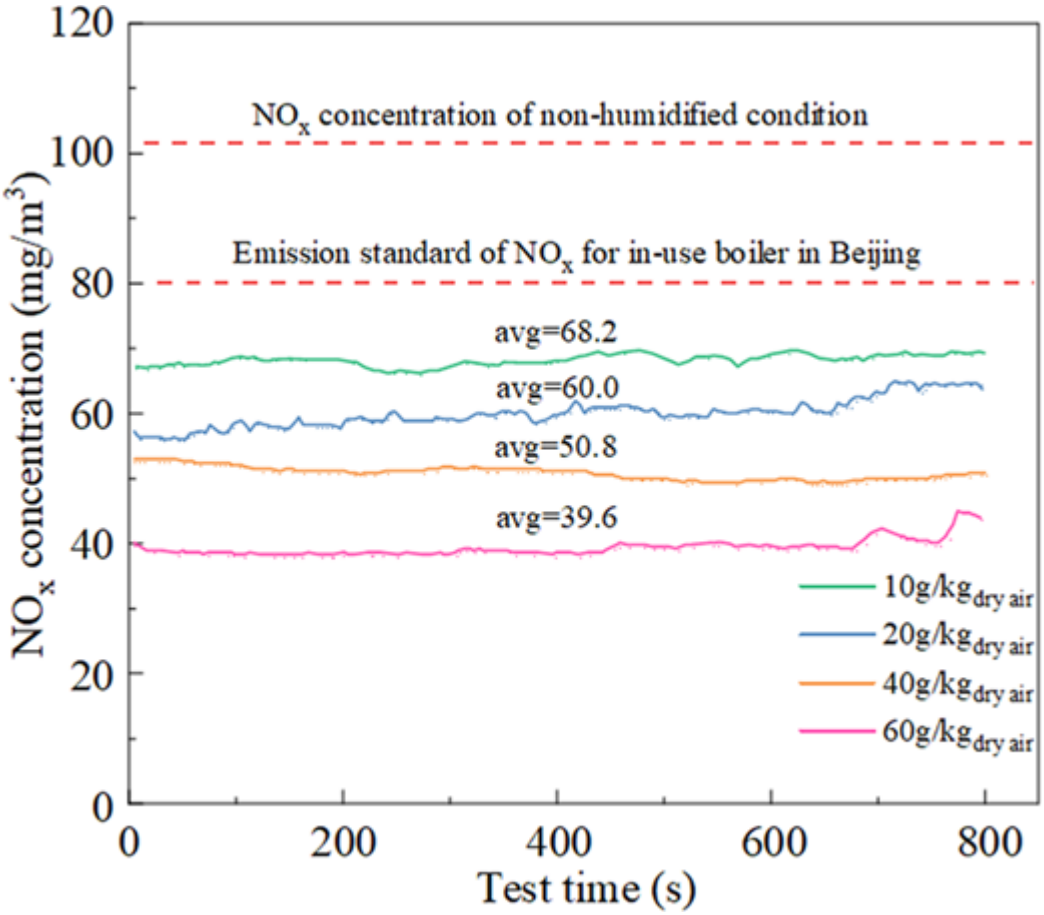

Fig. 11. Test chart of NO_x emission variance over time

The total NO_x emissions of the three systems when generating 1 GJ of heat are shown in Fig. 12. The NO_x emissions of the FGTHR system are 31.1 g lower than the original system, which is a relative reduction of 64.5%. The NO_x emissions of the FGTHR system are 28.7 g lower than those of the DCHE system, which is a relative reduction of 62.7%. The main reasons for the decrease in NO_x concentration are as follows: First, the fuel consumption of the FGTHR system is less than the original system. The FGTHR system has a better energy-saving performance. Second, the SW can purify the flue gas, which can eliminate the majority of NO_2. This is because NO is more easily soluble in water, but the NO_2 in flue gas is lower, accounting for about 5% of total NO_x [42]. Third, the SW in the combustion air evaporates and absorbs heat during combustion, which decreases the maximum flame temperature [31]. When the combustion air is not humidified, the maximum combustion temperature is 2250 K, and the furnace outlet temperature is 1620 K. When combustion air

humidity ratio is 60 g/kg$_{dry\ air}$, the highest combustion temperature is 2100 K, and the furnace outlet temperature is 1650 K.

(2) CO_2 emissions

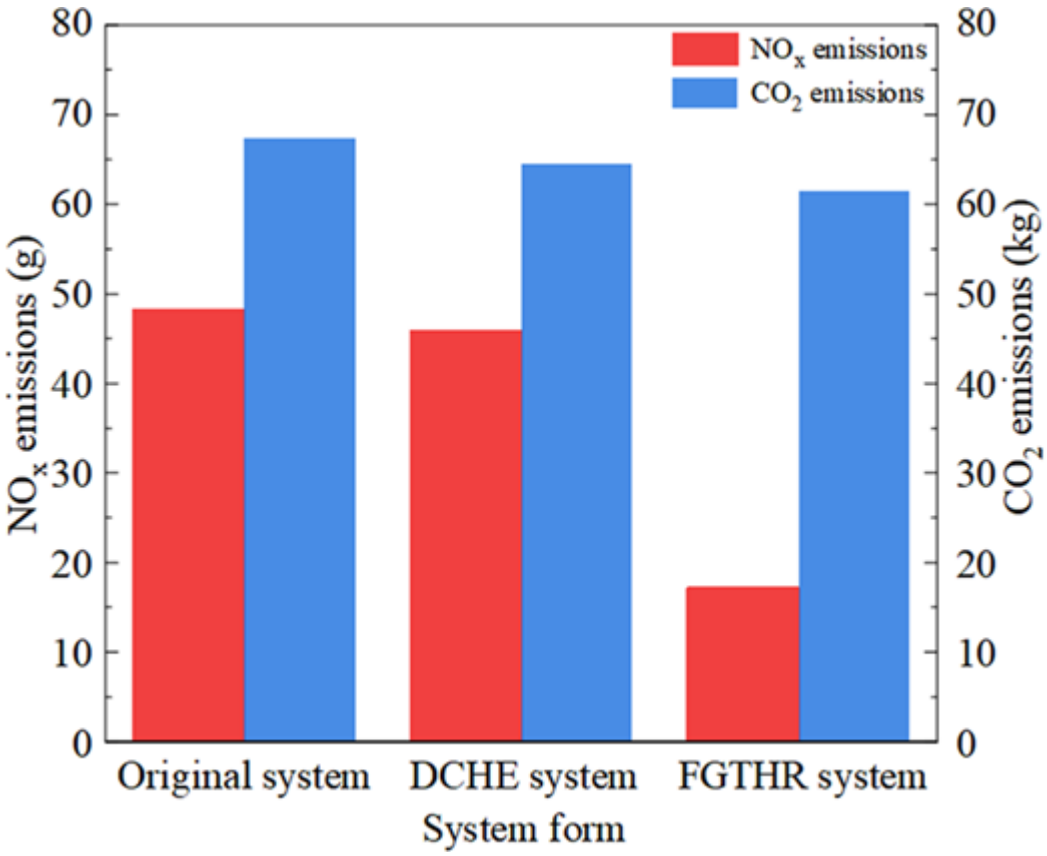

Fig. 12. Comparison between NO_x emissions and CO_2 emissions of three systems when generating 1 GJ of heat

The total CO_2 emissions of the different systems are shown in Fig. 12. The CO_2 emissions of the FGTHR system are 5.85 kg lower than the original system, which is a reduction of 8.7%. The CO_2 emissions of the FGTHR system are 2.93 kg lower than those of the DCHE system, which is a reduction of 4.5%. The reduction of CO_2 emissions in the FGTHR system is major caused by the energy savings of the FGTHR system. As can be seen above, the FGTHR system has better environmental benefits.

3.4 Comparison With Existing Waste Heat Recovery and Low-NO_x Technology.

The different technical methods of boiler WHR and low-NO_x emissions are shown in Fig. 13 for better comparisons. The recent research on gas boilers is compared with the results obtained for the proposed system in Table 6. It can be seen from Fig. 13 and Table 6 that the use of heat pump and the non-DCHE can achieve higher energy efficiency improvement, but the initial investment of the heat pump is high, and the non-DCHE also has corrosion problems, and neither of them can achieve NO_x emissions reduction. Commonly used low-NO_x combustion technologies can significantly reduce NO_x emissions with low initial investment, but hard to achieve energy efficiency improvements, and even reduce boiler efficiency. Comprehensively, the FGTHR system performs quite well among these systems.

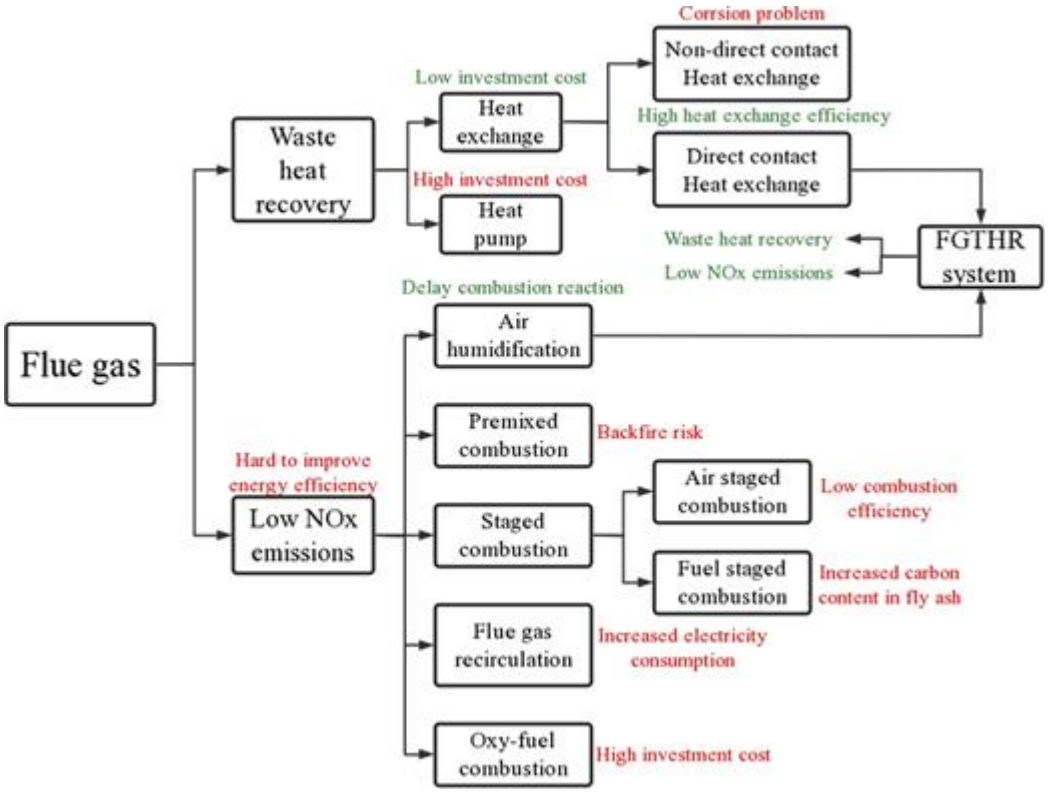

View largeDownload slide

Fig. 13. WHR and low-NO_x emissions technology methods flowchart

Table 6 Comparison between FGTHR system and the existing system of gas boilers

Researchers	Technology methods	Efficiency	NO_x emissions
Li et al. [43]	Absorption heat pump and DCHE	Improved 11.54%	34 ppm
Yang et al. [44]	Full-open absorption heat pump	Improved 0.436–0.632	–
Shang et al. [13]	Non-DCHE+ air humidification	Improved 13.4%	–
de Almeida and Lacava [45]	Double-stage swirl combustor	–	23 ppm
Lee et al. [46]	Multi-hole premixed	–	40 ppm
This paper	DCHE+ air humidification	Improved 8.4%	39.6 mg/m^3

3.5 Case Analysis for Waste Heat Recovery System Pollutants Diffusion

3.5.1 Case Description.

Since NO is unstable and ultimately oxidized by O_2 to NO_2, NO_2 is calculated approximately as NO_x. We took a WHR gas boiler as a model to analyze, which has the following characteristics:

1. The heating capacity of the boiler is 15 MW;
2. The emission rate of flue gas is 28,230 m^3/h;
3. The boiler outlet NO_x concentrations are 40 mg/m^3 (low-NO_x combustion mode) and 80 mg/m^3 (non-nitrogen combustion mode);

4. The chimney height is 8 m;
5. The chimney outlet diameter is 1.1 m; and
6. The area is a residential community in Beijing, China.

3.5.2 Exhaust Flue Gas Temperature Analysis.

The relationship between concentration and distance under different exhaust flue gas temperatures is shown Fig. 14. As the exhaust flue gas temperature is decreased from 90 °C to 30 °C, the max ground concentration of NO_x is increased from 157.7 $\mu g/m^3$ to 265.3 $\mu g/m^3$, and the ground distance is shortened from 33 m to 28 m. At the distance of 1200 m, the ground concentration of NO_x under different exhaust gas temperatures is basically the same, tending to a lower value. When the concentration of NO_x at the outlet is 80 mg/m^3, the exhaust gas temperature of 30 °C causes the ground concentration to exceed the standard. This is because the decrease in exhaust flue gas temperature will lead to a decrease in diffusion uplift capacity, which is not conducive to the diffusion of pollutants.

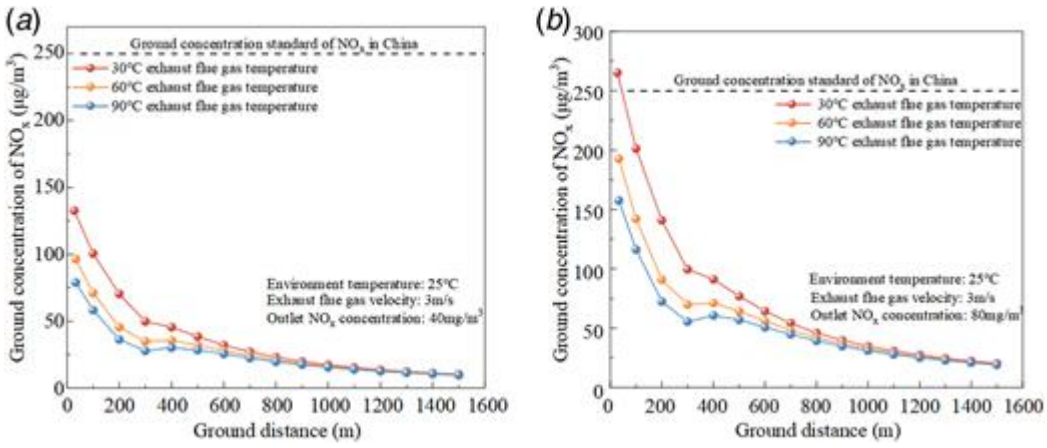

Fig. 14. The relationship between concentration and distance under different exhaust flue gas temperature

3.5.3 Exhaust Flue Gas Velocity Analysis.

Figure 15 shows the simulation results for the variation in exhaust flue gas velocity. As the exhaust flue gas velocity was decreased from 4 m/s to 2 m/s, the max ground concentration of NO_x increased from 216.2 $\mu g/m^3$ to 381.9 $\mu g/m^3$, and the ground distance increased from 31 m to 33 m. At the distance of 1100 m, the ground concentration of NO_x under different exhaust flue gas temperatures is basically the same, tending to a lower value. When the concentration of NO_x at the outlet is 80 mg/m^3, the exhaust flue gas velocity of 2 m/s and 3 m/s causes the ground concentration to exceed the standard. As a result, when the concentration of NO_x is 80 mg/m^3, the exhaust flue gas velocity of the SW tower should be kept above 4 m/s, and a gradually shrinking port should be retrofitted at the top of the SW unit to appropriately increase the velocity to ensure that the ground concentration less than 250 $\mu g/m^3$.

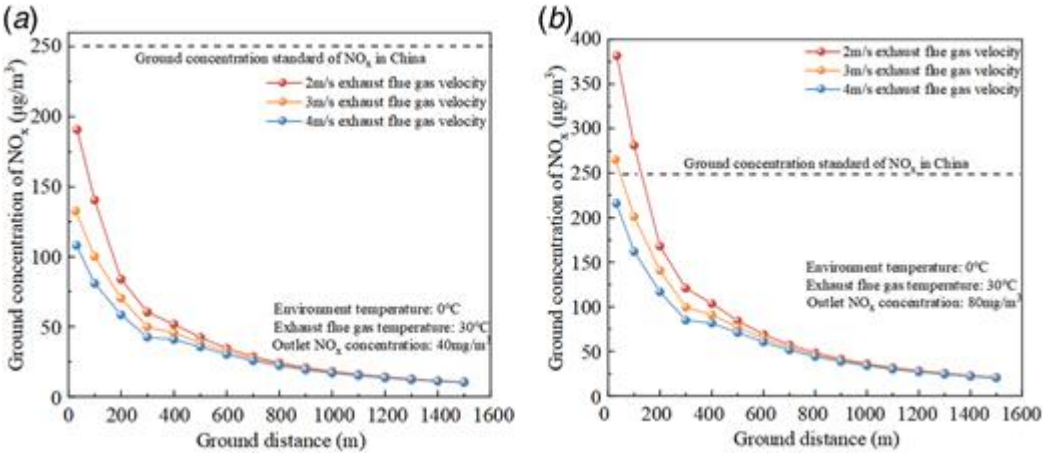

Fig. 15. The relationship between concentration and distance under different exhaust flue gas velocity

3.5.4 Exhaust Flue Gas Humidity Analysis.

A high SW flowrate can increase the flue gas humidity, and higher relative humidity is conducive to haze and smoke [47,48]. An increase in exhaust flue gas humidity will increase its density, weaken its vertical diffusion, and lead to the accumulation of pollutants in the near-surface layer. Humidity also hinders the diffusion of smoke and reduces the self-clearance rate of aerosols, leading to continuous haze weather. Similarly, excessive flue gas humidity can shorten the service life of pipelines and chimneys, leading to unstable operation of fans.

3.5.5 Countermeasures of Pollutants Diffusion Analysis.

To address the above issues, many countries have mandated the minimum exhaust flue gas temperature [49]. For instance, Japan requires exhaust flue gas temperatures to be between 90 °C and 100 °C, and practically all thermal power stations have flue gas reheaters installed. In the United States, some thermal power plants also use natural gas to preheat flue gas for emissions, but the increase in gas consumption leads to higher operating costs. All power plants have adopted high-temperature emissions, and some have added flue gas reheaters. Flue gas reheaters were frequently used for heating in the UK, where the temperature of flue gas emissions must not be lower than 80 °C. Gas–gas and water–gas heaters are the two types of flue gas heaters. The goal is to raise the flue gas's lifting height and stop low-temperature, wet flue gas from corroding the chimney's inner walls and flue. The emission temperature must not be less than 72 °C in Germany. Other flue gas heating techniques were encouraged in addition to building flue gas reheaters, and the flue gas is heated by leftover heat from cooling towers. Unlike conventional reheater methods, flue gas is not discharged through the chimney and is sent to a naturally ventilated cooling tower. The use of hot and humid air to form a gas curtain can generate huge thermal buoyancy and elevate the lifting height of the exhaust flue gas [6]. Heating the flue gas with residual heat from the cooling tower can eliminate the costly reheating system and significantly reduce the ground's average concentration of emissions.

4 Conclusion and Future Work

To collaboratively decrease high NO_x emission concentrations and increase boiler thermal efficiency of gas-fired boilers, the FGTHR system is put forward, which can decrease NO_x emissions without reducing heat efficiency. The conclusions can be given as below:

1. For the DCHE system, the dew point temperature of flue gas is 49.2 °C. When the combustion air humidity ratio is 60 $g/kg_{dry\ air}$, the dew point temperature of flue gas reaches 57.2 °C. Raising the temperature and humidity of the combustion air helps to increase the dew point temperature of the flue gas.
2. The quantity of WHR falls as the temperature of the SW rises and rises as the mass flowrate of the SW does. SW temperature has less of an effect on WHR than does SW quality flowrate. With SW flowrate and temperature of 0.075 kg/s and 45 °C, the WHR efficiency relatively increases by up to 8.4%.
3. Under the combustion air humidity ratio is 60 $g/kg_{dry\ air}$, the NO_x emissions averages 39.6 mg/m^3. NO_x and CO_2 emissions are reduced by 61.2% and 8.7% compared to non-CAH conditions.
4. The operating costs of the FGTHR system are 8.6% and 4.3% lower than the original system and DCHE system under generating generating 1 GJ of heat. The payback period of the FGTHR system is 2 years.
5. The decrease in exhaust flue gas temperature and velocity and the increase in exhaust flue gas humidity harm the diffusion of NO_x in the atmosphere. Flue gas heaters and cooling tower waste heat for heating flue gas are two techniques that can lower the average ground concentration of NO_x.

In the future, the research will mainly focus on the combustion mechanism (combustion temperature, combustion field stability, and combustion area). Meanwhile, air humidification technology will be combined with other low nitrogen methods such as air staged combustion to obtain a better low nitrogen emission effect.

Acknowledgment

We thank Tatiana Morosuk, Editor-in-Chief, ASME *Journal of Energy Resources Technology*, for her advice.

Funding Data

- The Fundamental Research Funds for Beijing University of Civil Engineering and Architecture (BUCEA).
- The BUCEA Post Graduate Innovation Project (PG2022070 and DG2023010).

Conflict of Interest

There are no conflicts of interest.

Data Availability Statement

The datasets generated and supporting the findings of this article are obtainable from the corresponding author upon reasonable request.

Nomenclature

CAH =combustion air humidification

CH_4 =methane

C_3H_8 =propane

CO_2 =carbon dioxide

DCHE =direct contact heat exchanger

fg =flue gas

FGTHR =flue gas total heat recovery

hw =heating water

ng =natural gas

N_2 =nitrogen

NO_X =nitrogen oxides

NO =nitric oxide

NO_2 =nitrogen dioxide

RH =relative humidity

RO_2 =triatomic gas

SO_2 =sulfur dioxide

SW =spray water

wp =water vapor

WHR =waste heat recovery

Symbols

d =humidity ratio, $g/kg_{dry\ air}$

m =mass flowrate, kg/s

t =temperature, °C

B =natural gas consumption, m^3/s

C =mass concentration, mg/m^3

M =relative molecular mass

Q =heat transfer, kw

V =volume of gas, m^3/m^3

C_w =constant pressure specific heat, kJ/kg · °C

E_t =cost of electricity, CNY

I_t =investment, CNY

P_t =payback period, a

S_t =cost-savings, CNY

net,ar =low calorific value

PPM =PPM concentration

α =excess air ratio

β =condensation rate of water vapor

ηb =boiler efficiency

ηt =total heat efficiency of boiler

References

[1] Tsoumalis, G. I., Bampos, Z. N., Chatzis, G. V., and Biskas, P. N., 2022, "Overview of Natural Gas Boiler Optimization Technologies and Potential Applications on Gas Load Balancing Services," Energies, 15(22), p. 8461.

[2] Kovacevic, M., Lambic, M., Radovanovic, L., Pekez, J., Ilic, D., Nikolic, N., and Kucora, I., 2017, "Increasing the Efficiency by Retrofitting Gas Boilers Into a Condensing Heat Exchanger," Energy Sources B: Econ. Plan. Policy, 12(5), pp. 470–479.

[3] Qureshi, Y., Ali, U., and Sher, F., 2021, "Part Load Operation of Natural Gas Fired Power Plant With CO2 Capture System for Selective Exhaust Gas Recirculation," Appl. Therm. Eng., 190, p. 116808.

[4] Yi, Z., Zhou, Z., Tao, Q., and Jiang, Z., 2019, "Experimental and Numerical Investigations in a Gas-Fired Boiler With Combustion Stabilizing Device," ASME J. Energy Resour. Technol., 141(11), p. 112201.

[5] Energy Institute, 2021, "BP Statistical Review of World Energy 2020 69th Edition," https://www.bp.com/en/global/corporate/energy-economics/statisticalreview-of-world-energy.html.

[6] Shuangchen, M., Jin, C., Kunling, J., Lan, M., Sijie, Z., and Kai, W., 2017, "Environmental Influence and Countermeasures for High Humidity Flue Gas Discharging From Power Plants," Renew. Sust. Energy Rev., 73, pp. 225–235.

[7] Cui, X. Y., Zhang, H. Y., Guo, J. F., Huai, X. L., and Xu, M., 2019, "Analysis of Two-Stage Waste Heat Recovery Based on Natural Gas-Fired Boiler," Int. J. Energy Res., 43(14), pp. 8898–8912.

[8] Kapustenko, P., Arsenyeva, O., Fedorenko, O., and Kusakov, S., 2022, "Integration of Low-Grade Heat From Exhaust Gases Into Energy System of the Enterprise," Clean Technol. Environ. Policy, 24(1), pp. 67–76.

[9] Ghobadi, J., Ramirez, D., Khoramfar, S., Jerman, R., Crane, M., and Hobbs, K., 2018, "Simultaneous Absorption of Carbon Dioxide and Nitrogen Dioxide From Simulated Flue Gas Stream Using Gas-Liquid Membrane Contacting System," Int. J. Greenh. Gas Control., 77, pp. 37–45.

[10] Paulauskas, R., Jogi, I., Striugas, N., Martuzevicius, D., Erme, K., Raud, J., and Tichonovas, M., 2019, "Application of Non-Thermal Plasma for NOx Reduction in the Flue Gases," Energies, 12(20), p. 3955.

[11] Jouhara, H., Bertrand, D., Axcell, B., Montorsi, L., Venturelli, M., Almahmoud, S., Milani, M., Ahmad, L., and Chauhan, A., 2021, "Investigation on a Full-Scale Heat Pipe Heat Exchanger in the Ceramics Industry for Waste Heat Recovery," Energy, 223, p. 120037.

[12] Murr, R., Ramadan, M., Khaled, M., and Olabi, A. G., 2019, “An Iterative Code to Investigate Heat Pump Performance Improvement by Exhaust Gases Heat Recovery,” Energy Sources A: Recovery Util. Environ. Eff., 41(18), pp. 2207– 2218.

[13] Shang, S., Li, X., Chen, W., Wang, B., and Shi, W., 2017, “A Total Heat Recovery System Between the Flue Gas and Oxidizing air of a Gas-Fired Boiler Using a Non-Contact Total Heat Exchanger,” Appl. Energy, 207, pp. 613–623.

[14] Xiong, Y., Tan, H., Wang, Y., Xu, W., Mikulcic, H., and Duic, N., 2017, “Pilot-Scale Study on Water and Latent Heat Recovery From Flue Gas Using Fluorine Plastic Heat Exchangers,” J. Cleaner Prod., 161, pp. 1416–1422.

[15] Zhang, Q., Niu, Y., Yang, X., Sun, D., Xiao, X., Shen, Q., and Wang, G., 2020, “Experimental Study of Flue Gas Condensing Heat Recovery Synergized With Low NOx Emission System,” Appl. Energy, 269, p. 115091.

[16] Pan, Q. W., Xu, J., Ge, T. S., and Wang, R. Z., 2022, “Multi-Mode Integrated System of Adsorption Refrigeration Using Desiccant Coated Heat Exchangers for Ultra-Low Grade Heat Utilization,” Energy, 238, p. 121813.

[17] Brueckner, S., Liu, S., Miro, L., Radspieler, M., Cabeza, L. F., and Laevemanna, E., 2015, “Industrial Waste Heat Recovery Technologies: An Economic Analysis of Heat Transformation Technologies,” Appl. Energy, 151, pp. 157–167.

[18] Dai, B., Liu, X., Liu, S., Zhang, Y., Zhong, D., Feng, Y., Nian, V., and Hao, Y., 2020, “Dual-Pressure Condensation High Temperature Heat Pump System for Waste Heat Recovery: Energetic and Exergetic Assessment,” Energy Convers. Manage., 218, p. 112997.

[19] Zhao, X., Fu, L., Wang, X., Sun, T., Wang, J., and Zhang, S., 2017, “Flue Gas Recovery System for Natural Gas Combined Heat and Power Plant With Distributed Peak-Shaving Heat Pumps,” Appl. Therm. Eng., 111, pp. 599–607.

[20] Wang, J., Hua, J., Fu, L., and Zhou, D., 2020, “Effect of Gas Nonlinearity on Boilersequipped With Vapour-Pump(BEVP) System for Flue-Gas Heat and Moisture Recovery,” Energy, 198, p. 117375.

[21] Yu, H. S., Gundersen, T., and Feng, X., 2018, “Process Integration of Organic Rankine Cycle (ORC) and Heat Pump for Low Temperature Waste Heat Recovery,” Energy, 160, pp. 330–340.

[22] Yang, B., Yuan, W., Fu, L., Zhang, S., Wei, M., and Guo, D., 2020, “Techno-Economic Study of Full-Open Absorption Heat Pump Applied to Flue Gas Total Heat Recovery,” Energy, 190, p. 116429.

[23] Kwon, M., Nguyen, B. H., Kim, S., Kim, Y., and Park, J. H., 2018, “Numerical Investigation of Buoyancy and Thermal Radiation Effects on a Mid-/Large-Sized Low NOx Combustion System With Flue-Gas Internal Recirculation,” Adv. Mech. Eng., 10(4), p. 168781401876913.

[24] Kikuchi, K., Murai, R., Hori, T., and Akamatsu, F., 2022, “Fundamental Study on Ammonia Low-NOx Combustion Using Two-Stage Combustion by Parallel Air Jets,” Processes, 10(1), p. 23.

[25] Jin, U., and Kim, K. T., 2022, “Influence of Radial Fuel Staging on Combustion Instabilities and Exhaust Emissions From Lean-Premixed Multi-Element Hydrogen/Methane/Air Flames,” Combust. Flame, 242, p. 112184.

[26] Sher, F., Pans, M. A., Sun, C. G., Snape, C., and Liu, H., 2018, “Oxy-Fuel Combustion Study of Biomass Fuels in a 20 kW(th) Fluidized Bed Combustor,” Fuel, 215, pp. 778–786.

[27] Zajemska, M., Musiał, D., and Poskart, A., 2014, “Effective Methods of Reduction of Nitrogen Oxides Concentration During the Natural Gas Combustion,” Environ. Technol., 35(5), pp. 602–610.

[28] Majdi Yazdi, M. R., Ommi, F., Ehyaei, M. A., and Rosen, M. A., 2020, “Comparison of Gas Turbine Inlet Air Cooling Systems for Several Climates in Iran Using Energy, Exergy, Economic, and Environmental (4E) Analyses,” Energy Convers. Manage., 216, p. 112944.

[29] Gascoin, N., Yang, Q. C., and Chetehouna, K., 2017, “Thermal Effects of CO2 on the NO Formation Behavior in the CH4 Diffusion Combustion System,” Appl. Therm. Eng., 110, pp. 144–149.

[30] Abdelaal, M., El-Riedy, M., El-Nahas, A. M., and El-Wahsh, F. R., 2021, “Characteristics and Flame Appearance of Oxy-Fuel Combustion Using Flue Gas Recirculation,” Fuel, 297, p. 120775.

[31] Pourhoseini, S. H., 2020, “Enhancement of Radiation Characteristics and Reduction of NOx Emission in Natural Gas Flame Through Silver-Water Nanofluid Injection,” Energy, 194, p. 116900.

[32] Feser, J. S., Gupta, A. K., and Amer Soc Mech, E., 2020, “Performance and Emissions of Drop-In Aviation Biofuels in a Lab Scale Gas Turbine Combustor,” Proceedings of the ASME Power Conference (POWER), Online, Aug. 4–5, p. V001T03A016.

[33] Ge, B., Tian, Y., and Zang, S., 2016, “The Effects of Humidity on Combustion Characteristics of a Nonpremixed Syngas Flame,” Int. J. Hydrog. Energy, 41(21), pp. 9219–9226.

[34] Vandel, A., Chica Cano, J. P., de Persis, S., and Cabot, G., 2022, “Study of the Influence of Water Vapour and Carbon Dioxide Dilution on Pollutants Emitted

by Swirled Methane/Oxygen-Enriched Air Flames," Exp. Therm. Fluid. Sci., 130, p. 110483.

[35] "The United States Environmental Protection Agency (EPA)," https://www.airnow.gov/, Accessed 2018.

[36] Ministry of Environmental Protection, 2012, GB/T 3095-2012. Beijing, Ministry of Environmental Protection, (in Chinese), http://www.syq.gov.cn/syq_doc/uploadfile/1448933137210.pdf.

[37] Wei, H., Huang, S., and Zhang, X., 2022, "Experimental and Simulation Study on Heat and Mass Transfer Characteristics in Direct-Contact Total Heat Exchanger for Flue Gas Heat Recovery," Appl. Therm. Eng., 200, p. 117657.

[38] Zuo, W., Zhang, X., and Li, Y., 2020, "Review of Flue Gas Acid DewPoint and Related Low Temperature Corrosion," J. Energy Inst., 93(4), pp. 1666–1677.

[39] Zhang, Q., Zhao, W., Sun, D., Meng, X., Hooman, K., and Yang, X., 2023, "Combustion Air Humidification for NOx Emissions Reduction in Gas Boiler: An Experimental Study," Heat Transf. Eng., pp. 1–14.

[40] Zhang, T., Zhou, Y., and Zhou, B., 2022, "The Effects of the Initial NO Volume Fractions on the NOx Generation and Reduction Routes Under Natural Gas MILD Combustion Conditions," Fuel, 328, 125175.

[41] Chen, H., Xie, B., Ma, J., and Chen, Y., 2018, "NOx Emission of Biodiesel Compared to Diesel: Higher or Lower?," Appl. Therm. Eng., 137, pp. 584–593.

[42] Li, Z., Hu, R., Xie, P., Chen, H., Liu, X., Liang, S., Wang, D., Wang, F., Wang, Y., Lin, C., Liu, J., and Liu, W., 2019, "Simultaneous Measurement of NO and NO2 by a Dual-Channel Cavity Ring-Down Spectroscopy Technique," Atmos. Meas. Tech., 12(6), pp. 3223–3236.

[43] Li, F., Lin, D., Fu, L., and Zhao, X., 2019, "Application of Absorption Heat Pump and Direct-Contact Total Heat Exchanger to Advanced-Recovery Flue-Gas Waste Heat for Gas Boiler," Sci. Technol. Built Environ., 25(2), pp. 149–155.

[44] Yang, B., Jiang, Y., Fu, L., and Zhang, S., 2018, "Experimental and

Theoretical Investigation of a Novel Full-Open Absorption Heat Pump Applied to District Heating by Recovering Waste Heat of Flue Gas," Energy Build., 173, pp. 45–57.
[45] de Almeida, D. S., and Lacava, P. T., 2015, "Analysis of Pollutant Emissions in Double-Stage Swirl Chamber for Gas Turbine Application," Proceedings of the 12th International Conference on Combustion and Energy Utilisation (ICCEU), Lancaster, UK, Sept. 29–Oct. 3, 2014, pp. 117–120.
[46] Lee, S., Kum, S.-M., and Lee, C.-E., 2011, "An Experimental Study of a Cylindrical Multi-Hole Premixed Burner for the Development of a Condensing Gas Boiler," Energy, 36(7), pp. 4150–4157.
[47] Tian, Y. L., Zhang, L. N., Wang, Y., Song, J. X., and Sun, H. T., 2021, "Temporal and Spatial Trends in Particulate Matter and the Responses to Meteorological Conditions and Environmental Management in Xi'an, China," Atmosphere, 12(9), p. 1112.
[48] Hua, Y., Wang, S., Jiang, J., Zhou, W., Xu, Q., Li, X., Liu, B., Zhang, D., and Zheng, M., 2018, "Characteristics and Sources of Aerosol Pollution at a Polluted Rural Site Southwest in Beijing, China," Sci. Total Environ., 626, pp. 519–527.
[49] China Control Engineering, 2015, "Uncovering the Truth of Smog: Ignoring the Temperature and Humidity of Emitted Smoke," http://www.cechina.cn/.